A Floating Self-Assembly Route to Colloidal Crystal Templates for 3D Cell Scaffolds

Yuanfang Liu,[†] Shaopeng Wang,*[,†] Jung Woo Lee,[‡] and Nicholas A. Kotov[‡,§]

Nomadics, Inc., 1024 South Innovation Way, Stillwater, Oklahoma 74074, and Departments of Biomedical Engineering, of Chemical Engineering, and of Materials Science, University of Michigan, 2300 Hayward, Ann Arbor, Michigan 48109

Received November 7, 2004. Revised Manuscript Received August 2, 2005

Preparation of well-ordered three-dimensional (3D) scaffolds is of great importance for various aspects of tissue engineering and fundamental research in cell biology. A versatile technique, floating self-assembly, is reported here for the first time to prepare 3D colloidal crystals from polystyrene particles of various diameters (10−240 μm). Ethylene glycol was used as the solvent in the self-assembly process of colloidal crystals. Polymer colloidal particles float on the surface of ethylene glycol and self-assemble into a hexagonal crystal lattice structure. The slow evaporation of ethylene glycol left solvent-free 3D colloidal crystals. Na_2SiO_3 sol−gel solution was infiltrated into the interstitial space of the prepared colloidal crystals, taking advantage of the capillary effect, and an inverse opal with a highly ordered system of spherical cavities interconnected by channels was obtained by calcining the colloidal particles at high temperature. As-prepared inverse opals were used as 3D cell scaffolds which possess a high degree of order compared to existing foamlike and fibrous cell scaffolds and afford tight control over the scaffolds' porosity and tissue organization. Their preparation by this technique is much simpler than that by free-form fabrication techniques. The biocompatibility of the prepared cell scaffolds is demonstrated through human hepatocellular carcinoma HEP G2 and human bone marrow HS-5 cell cultures.

1. Introduction

Three-dimensional (3D) colloidal crystals and their corresponding inverse opals have a variety of potential applications in electro- and nonlinear optics, optical and magnetic information processing and storage, catalysis, sensors, optical switches, etc.[1−3] The most discussed potential application of 3D colloidal crystals is based on the photonic band gap property.[4,5] For the preparation of 3D colloidal crystals with different sizes, several approaches such as solvent evaporation, sedimentation, physical confinement, filtration and pressing, membrane filtration, emulsion crystallization, and the Langmuir−Blodgett (LB) method have been used.[6−13] The assembly of solvent-free colloidal crystals is the basis for obtaining highly ordered 3D inverse opals. A common approach to fabricate these structures is to use the colloidal crystals as the template, fill the interstitial spaces between the colloidal spheres with another material, and then selectively remove the spheres by chemical etching or calcinations.[14−16] So far, colloidal crystals have been prepared from nanosized and submicrometer-sized colloidal particles, and the application of inverse opals was mainly focused on photonic crystals and photonic band gap materials. We are interested in extending the use of the unique ordering of the colloidal crystals and their inverse replica beyond utilization of the photonic band gap, for instance as promising cell scaffolds[20] with a potential for systematic study of the effects of 3D order on cell interactions.

The existing 3D cell scaffolds have several drawbacks with respect to protocols for cell culturing as well as replication of the actual 3D environment of the tissue. Yang et al.

* To whom correspondence should be addressed. E-mail: swang@nomadics.com.

[†] Nomadics, Inc.

[‡] Department of Biomedical Engineering, University of Michigan.

[§] Departments of Chemical Engineering and of Materials Science, University of Michigan.

(1) Zeng, F.; Sun, Z. W.; Wang, C. Y.; Ren, B. Y.; Liu, X. X.; Tong, Z. *Langmuir* **2002**, *18*, 9116.
(2) Joannopoulous, J. D.; Villeneuve, P. R.; Fan, S. *Nature* **1997**, *386*, 143.
(3) Reese, C.; Mikhonin, A.; Kamenjicki, M.; Tikhonov, A.; Asher, S. A. *J. Am. Chem. Soc.* **2004**, *126*, 1493.
(4) Yablonovith, E. *Phys. Rev. Lett.* **1987**, *58*, 2059.
(5) Krauss, T. F.; De La Rue, R. M. *Prog. Quantum Electron.* **1999**, *23*, 51.
(6) Park, S. H.; Xia, Y. *Langmuir* **1999**, *15*, 266.
(7) Park, S. H.; Qin, D.; Xia, Y. *Adv. Mater.* **1998**, *10*, 1028.
(8) Jiang, P.; Bertone, J. F.; Hwang, K. S.; Colvin, V. L. *Chem. Mater.* **1999**, *11*, 2132.
(9) Donselaar, L. N.; Philipse, A. P.; Suurmond, J. *Langmuir* **1997**, *13*, 6018.
(10) Zhou, Z. C.; Zhao, X. S. *Langmuir* **2004**, *20*, 1254.
(11) Gates, B.; Qin, D.; Xia, Y. *Adv. Mater.* **1999**, *11*, 466.
(12) Velev, O. D.; Lenhoff, A. M.; Kaler, E. W. *Science* **2000**, *287*, 2240.
(13) Im, S. H.; Kim, M. H.; Park, O. O *Chem. Mater.* **2003**, *15*, 1797.
(14) Holland, B. T.; Blanford, C. F.; Stein, A. *Science* **1998**, *281*, 538.
(15) Salgueiriño-Maceira, V.; Rodríguez-González, B.; Hellweg, T.; Liz-Marzán, L. M. *Aust. J. Chem.* **2003**, *56*, 1017.
(16) Jiang, P.; Hwang, K. S.; Mittleman, D. M.; Bertone, J. F.; Colvin, V. L. *J. Am. Chem. Soc.* **1999**, *121*, 11630.
(17) Yang, S.; Leong, K. F.; Du, Z.; Chua, C. K. *Tissue Eng.* **2002**, *8*, 1.
(18) Liu, Y. F.; Wang, S. P.; Kotov, N. A.; Cumming, C.; Motamedi, M.; Nichols, J. E.; Cortiella, J. *Abstracts of Papers*, 227th ACS National Meeting; American Chemical Society: Washington, DC, 2004; PMSE-264.
(19) Wang, S. P.; Liu, Y. F.; Kotov, N. A.; Mamedov, A.; Westcott, S.; Cumming, C.; Nichols, J. E.; Cortiella, J.; Motamedi, M. *Abstracts of papers*, 227th ACS National Meeting; American Chemical Society: Washington, DC, 2004; PMSE 454.
(20) Kotov, N. A.; Liu, Y. F.; Wang, S. P.; Cumming, C.; Eghtedari, M.; Vargas, G.; Motamedi, M.; Nichols, J.; Cortiella, J. *Langmuir* **2004**, *20*, 7887.

10.1021/cm048050g CCC: $30.25
Published on Web 09/10/2005

pointed out that tissue engineering on them is less than ideal for actual applications because of the lack of mechanical strength, interconnected channels, and controlled porosity or pore distribution.[17] A possible solution is to take advantage of inverse colloidal crystals with suitable material composition as cell scaffolds. Here, a simple mixed-solvent evaporation technique to produce 3D colloidal crystals is demonstrated, which allows the preparation of colloidal crystals from large spherical colloids faster than the previous approach.[18−20] Floating self-assembly is a fast method used to prepare colloidal crystals with polystyrene colloidal particles of different diameters, such as 10, 80, 160, and 240 μm. Subsequently, they were transformed into inverted replicas, and highly ordered porous 3D scaffolds that resemble the geometry of bone marrow were produced. Successful culture of human hepatocellular carcinoma HEP G2 and human bone marrow HS-5 stromal cells demonstrated that these 3D scaffolds are biocompatible.

2. Experimental Section

2.1. Preparation of Colloidal Crystals and 3D Cell Scaffolds. A 10 ± 0.74 μm 4.2% white sulfate latex aqueous suspension was purchased from Interfacial Dynamics. An 80 ± 0.8 μm 1.8% polystyrene microspheres aqueous suspension, a 160 ± 2.4 μm 5.0% polymer microspheres aqueous suspension, and 240 ± 9.2 μm solid polymer microspheres were purchased from Duke Scientific. Na_2SiO_3 sol−gel (Si content 1 mg/mL) was purchased from Fisher Scientific. Ethylene glycol was purchased from Aldrich. The concentration of 10, 80, and 160 μm colloidal particles was adjusted to about 10 wt % by extracting the water in the aqueous suspension before use. The typical experiment is as follow: A simple vial was made by gluing a plastic tube of 8 mm diameter onto a plastic plate. The vial was half-filled with ethylene glycol first. Then the polymer colloidal particle solution was taken into a pipet, and the colloidal particles were allowed to settle to the bottom part of the pipet by gravity before being dropped into the container, since the density of the colloidal particles (1.05 g/cm) is slightly larger than the density of water (1.0 g/m). In this way, the colloidal particles were dropped into the vial while most of the water was left behind. The final volume of the colloidal particles in the vial is about equal to the volume of ethylene glycol. Next, the container was placed in a 5 cm diameter dish covered with porous aluminum foil and was heated at 100 °C in an oven to allow the solvent to evaporate. The solvent was evaporated completely, and colloidal crystals were obtained after 3 h. The procedure was virtually identical for colloidal particles of all diameters. To get inverse opals, the colloidal crystals were infiltrated with Na_2SiO_3 sol that was diluted with an equal volume of deionized water. The composite colloidal crystals were dried in air for 12−24 h to allow the Na_2SiO_3 sol to become a gel. After the crystals were heated at 600 °C in the air for 10 min, the colloidal crystal templates were burned away and 3D scaffolds were obtained.

2.2. Cell Cultures. Human hepatocellular carcinoma HEP G2 (CRL-11997) and human bone marrow stromal HS-5 (CRL-11882) cells were purchased from American Type Culture Collection (ATCC). ATCC recommended media were used to culture the cells.[20] For HEP G2, a 1:1 mixture of Dulbecco's modified Eagle's medium and Ham's F12 medium with 2.5 mM L-glutamine, 15 mM HEPES, 0.5 mM sodium pyruvate, and 1200 mg/L sodium bicarbonate and supplemented with 0.4 mg/mL G418 (antibiotic) and 10% fetal bovine serum was used. For HS-5: Dulbecco's modified Eagle's medium with 4 mM L-glutamine, 4.5 g/L glucose, and 1.5 g/L sodium bicarbonate (ATTC 30-2002) and supplemented with 10% fetal bovine serum (ATCC 30-2021) and 1% penicillin−streptomycin (Sigma P3539) was used. Both cell lines were cultured and maintained in 25 cm^2 cell culture flasks at 37 °C with 5% CO_2, split rate 1:4 to 1:6 for HEP G2 and 1:6 to 1:10 for HS-5. The scaffolds were placed in a 96-well cell culture plate, seeded with 10^4 to 10^5 cells per well in 0.25 mL of medium, and incubated at 37 °C, 5% CO_2. The media were changed every 2−4 days.

2.3. Measurements. Scanning electron microscopy (SEM) images were obtained with a JEOL JXM 6400 scanning electron microscope with an Oxford X-ray system and cryostage and equipped with a Zeiss CCD imaging package. For a scaffold with cells, the samples were chemically fixed according to the standard procedure for tissue fixation. In brief this procedure includes the following steps: (a) glutaraldehyde (GA) fixation for at least 12 h, (b) 0.1% GA buffer wash three times for 20 min each, (c) osmication treatment with OsO_4 for 2 h, (d) 0.1% GA buffer wash to remove the remaining osmium oxide three times for 20 min each, (e) dehydration steps with 50%, 70%, 90%, and 95% ethanol washes for 20 min each, followed by 100% ethanol wash three times for 20 min each, (f) critical point drying. Prior to imaging, the fixed scaffolds were coated with gold using a Denton Desktop II sputter coater (Denton Vacuum, Inc.).

Confocal microscopy was carried out on a Leica SP2 confocal microscope with and 20× objectives and a 488 nm laser as the excitation source. The images were obtained for emission collected in a 515−550 nm spectral window. The cells on the scaffold were stained with carboxyfluorescein diacetate, succinimidyl ester (CFSE; Molecular Probes Inc., V-12883). Scaffolds with cells were transferred to a 24-well microplate with 1 mL of 1 μM CFSE diluted in PBS buffer and incubated at 37 °C for 15 min. After that, the medium was washed with 1 mL of PBS and then replaced with fresh medium. The cells were incubated for at least 30 min longer prior to imaging.

3. Results and Discussion

The ordered structure of the as-prepared colloidal crystals and scaffolds was determined with SEM images, as shown in Figure 1. One can see that 10, 80, 160, and 240 μm polymer colloidal particles can assemble into close-packed 3D colloidal crystals. The corresponding scaffolds, which are shown as insets, have a degree of ordered structure similar to that of the original templates. The diameter of the cavities corresponds very well with the diameter of the starting colloidal spheres except it is 5−10 μm smaller for $d = 160$ μm and $d = 240$ μm. The scaffolds have interconnection channels 5−80 μm in diameter between cavities as well, which is important for the transfer of nutrients and the migration of cells. The geometry of the cavities and the interconnection channels is distorted compared to that of the ideal inverted colloidal crystal, most likely due to heat treatment necessary to form silicate.

The SEM images in Figure 1 were taken from the surface of colloidal crystals in the tubes. To show the obtained colloidal crystals have 3D structure, we tried to get free-standing 3D colloidal crystals by the following method: we put the 80 μm colloidal crystals within the tube into a 600 °C oven for 1 min and then separated the colloidal crystals and tube rapidly with the aid of tweezers while the tube was still soft. The SEM image in Figure 2a indicates that the obtained colloidal crystals possess 3D ordered structure. The

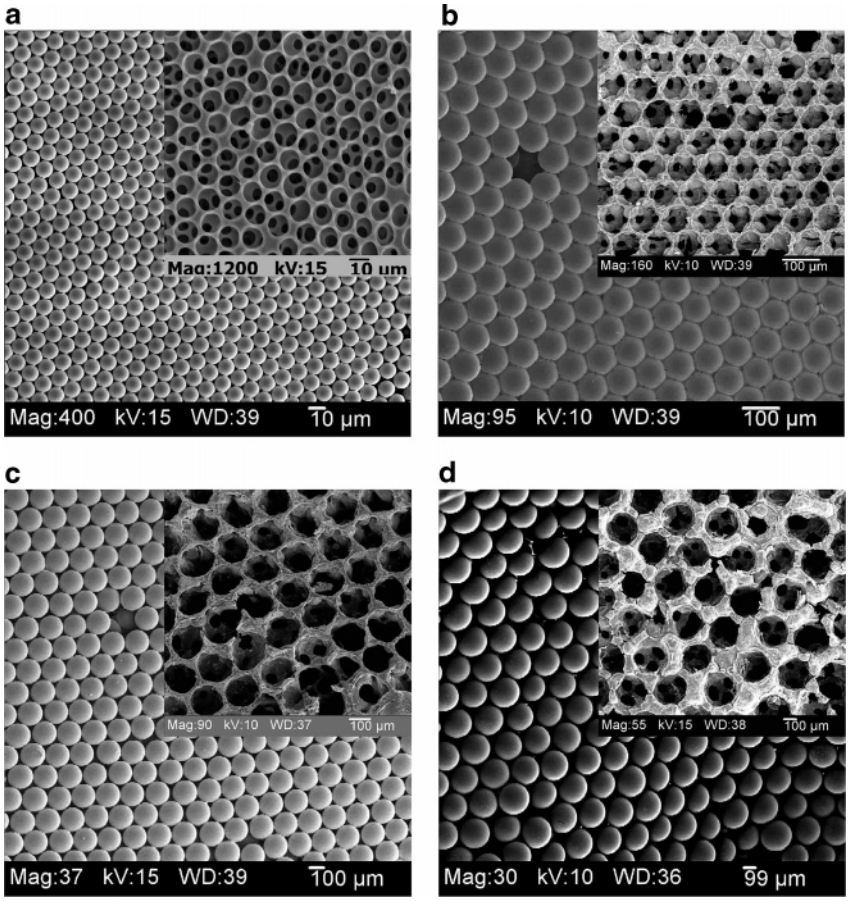

Figure 1. SEM images of colloidal crystals made from colloidal particles of diameter (a) 10 μm, (b) 80 μm, (c) 160 μm, and (d) 240 μm. Insets are the corresponding inverse opal structures.

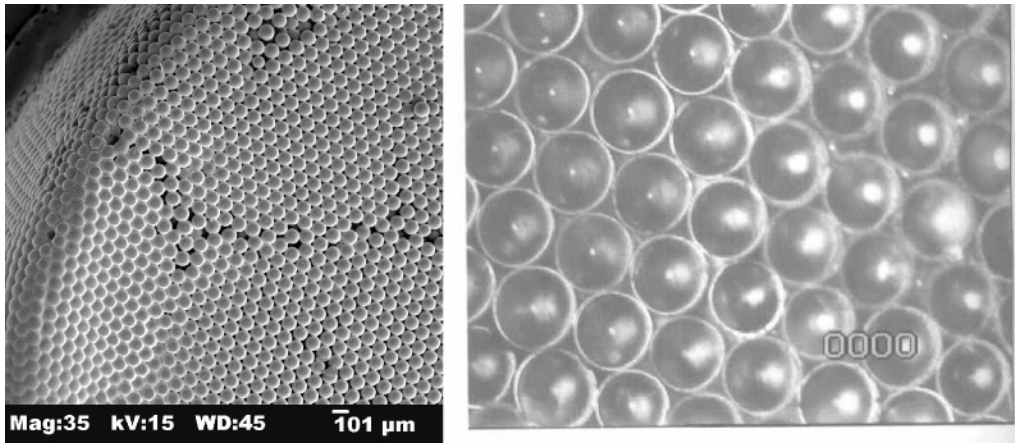

Figure 2. (a, left) SEM image of the 3D structure of 80 μm colloidal crystals. (b, right) Microscopy image of 240 μm polymer colloidal particles floating on the surface of ethylene glycol.

thickness L of the 3D colloidal crystals can be calculated by the geometry of 11 layers of 80 μm colloidal particles to be $L = 11 \times 80\ \mu\text{m} \times \sin 60° = 762\ \mu\text{m} = 0.76$ mm. The thickness can be adjusted through changing the amount of added microspheres.

This floating self-assembly technique has the following advantages over our former mixed-solvent evaporation (MSE) method:[18−20] (1) It can be used to prepare any size of colloidal crystals under exactly the same experimental parameters. We do not need to change the temperature and time of the crystal formation process for differently sized colloidal crystals as we do when using the MSE method. The versatility of this approach is superior to that of other colloidal crystal preparation methods considering the experimental parameters remain the same for all sizes of polymer microspheres. (2) The obtained colloidal crystals and scaffolds have better long-range order than those prepared through the MSE method.[20] (3) Ethylene glycol does not dissolve polystyrene microspheres even at a temperature as high as 130 °C, while pure DMF or high-concentration DMF aqueous solutions used in the MSE method can damage polystyrene microspheres at room temperature due to the high solvency of DMF for the polymer. (4) The experimental operation is much simpler and safer than MSE because

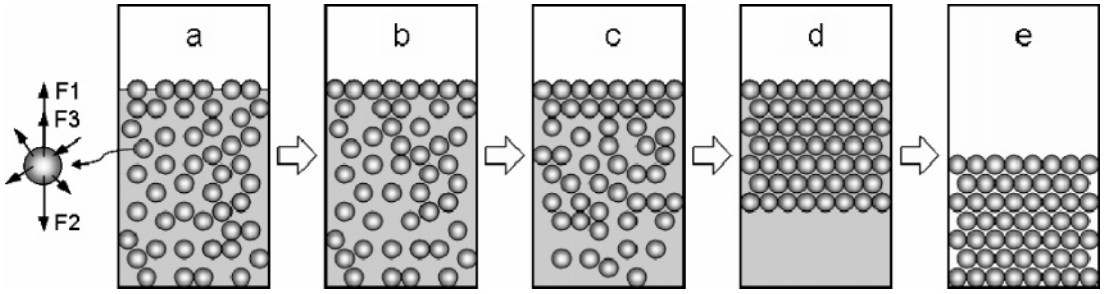

Figure 3. Schematics of the floating assembly process: (a) formation of a nucleus on the surface; (b) formation of the first layer of colloidal crystals; (c) formation of the second layer of colloidal crystals; (d) formation of the whole colloidal crystal; (e) solvent-free colloidal crystals. The forces applied to colloidal particles in the vertical direction are F1 (buoyancy), F2 (gravity), and F3 (immersion lateral capillary force); among them, F1 > F2 > F3. The forces in other directions are the floating lateral capillary force, electrostatic attractive force, and electrostatic repulsive force. The directions of these forces may change with the movement and position of the microspheres. They act together to make microspheres pack closely.

ethylene glycol is a low-vapor-pressure solvent compared to DMF. (5) Last but not least, it is faster. The floating self-assembly method only needs 3 h to obtain colloidal crystals, while the MSE method needs 3 days.

In the floating self-assembly process of colloidal crystals, the density of the solvent ethylene glycol plays an important role. The density $D_{\text{ethylene glycol}} = 1.11$ g/mL is higher than $D_{\text{polymer}} = 1.05$ g/mL. The polymer colloidal particles float on the surface of the ethylene glycol and self-assemble into 3D colloidal crystals, which can be observed under a microscope (shown in Figure 2b). Actually, floating self-assembly is a common natural phenomenon. As an example, oil droplets can float on the surface of water and self-assembly into an ordered structure. Another example is that soap bubbles can self-assemble into an ordered structure on the surface of water. The same principle governs Langmuir monolayers.[21] Here again the specific density D_{water} is higher than D_{oil} or $D_{\text{soap bubble}}$. As a matter of fact, these phenomena give us a good hint for developing this method of preparation of 3D colloidal crystals. After self-assembly into 3D colloidal crystals in ethylene glycol, the polymer microspheres can become solvent-free 3D colloidal crystals under slow to medium evaporation by controlling the evaporation temperature.

The floating assembly process is illustrated in Figure 3. During the assembly process, several forces govern the movement of the colloidal particles in the solution. In addition to buoyancy (F1) and gravity (F2), there are several kinds of interparticle forces once the particles are closely packed.[22−25] They are floating lateral capillary forces, immersion lateral capillary forces (F3), and electrostatic attractive and repulsive forces. The major forces in the vertical direction are F1, F2, and F3, and among them, F1 > F2 > F3, due to the higher density of ethylene glycol than the polymer colloidal particles. The directions of other forces change with the movement and position of the microspheres. All forces act together to make colloidal particles ascend and self-organize into ordered layers. Among them, the floating lateral capillary force acts on particles that are floating on the water surface. The immersion lateral capillary force acts on particles protruding out of the water surface. As the particles of the top layer protrude out of the latex surface under the effect of the buoyancy, gravity, and electrostatic repulsive forces from the particles of the second layer, a water meniscus[22] can probably be formed between particles, and thus, a strong capillary force will arise. The lateral projection of the capillary force is much stronger than that of the electrostatic repulsive force between the adjacent particles on the first layer and drags the particles together to form a crystal nucleus on the surface (Figure 3a). After that, driven by the buoyancy force, lateral capillary force, and convection force, the crystals grow on the first layer through directional motion of particles toward the closely packed nucleus (Figure 3b). The close-packed first layer acts as a template (seed of the crystal) to guide the close packing of underlayers in a layer by layer fashion, which is mainly driven by the buoyancy force (Figure 3c). Upon the formation of ordered layers, the Brownian motion of the colloidal particles significantly slows since the particles are almost fixed at a given position by the forces described above. As a result, the individual particles in the layered structure are unable to make long-range movement, and the ordered structure is kept; therefore, a floating 3D colloidal crystal forms (Figure 3d). Finally, solvent-free colloidal crystals are obtained by slow evaporation of solvent (Figure 3e). The self-assembly mechanism here is similar to that of 3D self-assembly of nanosized colloidal crystals in Park's work[26] except the up-force is different.

To investigate the role of the density difference between the solvent and the microspheres in the formation of colloidal crystals, mixtures of ethylene glycol and water with various volume ratios (1:1, 1:2, 1:3, and 1:4) are used to substitute for pure ethylene glycol, while keeping the temperature constant. In the case of the 1:1 mixture, the ordered colloidal crystals can form immediately on the surface of the mixture and very ordered solution-free colloidal crystals can be obtained after evaporation of the solvent. In the case of the 1:2 mixture, the ordered colloidal crystals can form on the surface of the mixture after about 2 h and the obtained solution-free colloidal crystals are very ordered as well. In the cases of the 1:3 and 1:4 mixtures, no ordered colloidal crystals form on the surface of the solution even after 4 h

(21) Gaines, G. L., Jr. *Insoluble monolayers at liquid-gas interfaces*; Wiley: New York, 1966.
(22) Kralchemsky, P. A.; Nagayama, K. *Langmuir* **1994**, *10*, 23.
(23) Denkov, N. D.; Velev, O. D.; Kralchevsky, P. A.; Ivznov, I. B.; Yoshimura, H.; Nagayama, K. *Langmuir* **1992**, *8*, 3183.
(24) Dimitrov, A. S.; Nagayama, K. *Chem. Phys. Lett.* **1995**, *243*, 462.
(25) Rakers, S.; Chi, L. F.; Fuchs, H. *Langmuir* **1997**, *13*, 7121.
(26) Im, S. H.; Lim, Y. T.; Suh, D. J.; Park, O. O. *Adv. Mater.* **2002**, *14*, 1367.

Table 1. Effect of the Solution Density on Colloidal Crystal Formation

ratio of water and ethylene glycol	0:1	1:1	1:2	1:3	1:4
density of the mixture solution (g/mL)	1.11	1.099	1.07	1.05	1.04
density of the microspheres (g/mL)	1.05	1.05	1.05	1.05	1.05
time of colloidal crystal formation on the surface of the solution	<2 min	~5 min	~2 h		
experimental temperature (°C)	75	75	75	75	75
quality of solution-free colloidal crystals	ordered	ordered	ordered	less ordered	less ordered

Table 2. Effect of Temperature on Colloidal Crystal Formation

temperature (°C)	60	70	80	90	100	110	130
evaporation time	4 days	2 days	1 day	12 h	3 h	2.5 h	1.5 h
quality of products	ordered	ordered	ordered	ordered	ordered	partially ordered	not ordered

and the obtained colloidal crystals are less ordered than those in the 1:1 and 1:2 mixtures.

To calculate the density of different solution mixtures, the volume of the different mixtures was measured with a 200−1000 μL pipet and a 0−250 μL syringe. We mixed 1 mL of ethylene glycol with 1, 2, 3, and 4 mL of water, respectively. The volume of the mixture was measured as $V(1:1) = 1.92$ mL, $V(1:2) = 2.90$ mL, $V(1:3) = 3.91$ mL, and $V(1:4) = 4.90$ mL. The density of water $D_1 = 1$ g/mL, and the density of ethylene glycol $D_2 = 1.11$ g/mL. Therefore, the density of the mixtures D can be calculated as $D = (D_1V_1 + D_2V_2)/V$, where V is the volume of the mixed solution. The calculated results are the following: $D(1:1) = 1.099$ g/mL, $D(1:2) = 1.07$ g/mL, $D(1:3) = 1.05$ g/mL, and $D(1:4) = 1.04$ g/mL.

The effect of the solution density is listed in Table 1. By comparing the results and the density of the mixed solution, we can come to the following conclusions: (1) A higher density difference between the solvent and microspheres contributes to a faster formation of ordered structure. (2) When the density of the solution is higher than the density of the microspheres, the order degree of same-sized colloidal crystals is the same for various density differentials. For a macroobject, one can calculate the time of flotation through the following parameters: gravity, buoyancy, volume of the object, density of the fluid and the object, and acceleration and distance of the object movement. Other forces, such as the immersion lateral capillary force, floating lateral capillary force, electrostatic attractive force, and electrostatic repulsive force, are relatively small compared to gravity and buoyancy; therefore, they may be ignored. For a microobject, we need to consider all of these forces. It is important to remember this for the qualitative assessments, although the actual modeling on their basis is difficult. In part this is due to the fact that these forces vary in direction and magnitude when the microspheres are in different positions, which leads to the different accelerations of the microspheres.

To further verify the effect of the density difference on the formation of 3D colloidal crystals, we employed uniform-sized soda lime glass colloidal particles, which have a density of 2.45 g/ml, to replace polystyrene colloidal particles while keeping other experimental conditions identical. The resulting colloidal crystals are not ordered. When diiodomethane ($D = 3.33$ g/mL, bp = 181 °C) was used as the solvent to prepare colloidal crystals from glass colloidal particles at room temperature, 50 °C, 60 °C, and 70 °C, good ordered colloidal crystals were obtained. These results further confirm that the high density difference between the solvent and microspheres is beneficial to the formation of a well-ordered structure. Park[26] put forward that the effective density of the assembled particles is lower than the density of water, causing particles to float on the water surface for the 3D self-assembly of 240−900 nm colloidal crystals. An effort was made to prepare 3D colloidal crystals from 10−240 μm microspheres by using Park's method, but this attempt failed.

Temperature is another important factor affecting the process of self-assembly of colloidal crystals. A lower temperature resulted in slower evaporation of solvent and a longer time to obtain the solvent-free colloidal crystals. A higher temperature may destroy the ordered structure of 3D colloidal crystals because of the rapid evaporation of solvent and the coalescence of polystyrene microspheres above its T_g, which is ca. 100 °C. Keeping other experimental parameters identical (160 μm polystyrene colloidal particles and ethylene glycol were used in the experiments), the experiments were conducted at 60, 70, 80, 90, 100, 110, and 130 °C. In the cases of 60−100 °C, the obtained colloidal crystals are very ordered but the times of solvent evaporation to get solvent-free colloidal crystals are quiet different. Those times are 4 days, 2 days, 1 day, 12 h, and 3 h for 60, 70, 80, 90, and 100 °C, respectively. The as-prepared colloidal crystals are partially ordered at 110 °C and the obtained structure is not ordered at 130 °C although the evaporation times are shorter. The experimental conditions of temperature and time of solvent evaporation and the experimental results are listed in Table 2. Considering the experimental time and quality of the products, the optimum temperature in our experiments is 100 °C.

The inverted colloidal crystals with $d > 10$ μm voids require a sol−gel preparation of greater strength than those typically made for photonic band gap studies. At the same time, a sol with high viscosity does not infiltrate uniformly into the colloidal crystals and can actually destroy them. When one adds the requirement of biocompatibility, finding a sol−gel formulation with the proper combination of all parameters becomes a research project with significant challenge. Among different sol−gel formulation tests based on titania and silica, it was found that a Na_2SiO_3 sol that consists of a 1:1 mixture of commercially available sodium silicate and deionized water can not only infiltrate into the colloidal crystals uniformly but also support the open structure with a large percentage of voids. To complete the inversion process, the organic colloid was completely removed by burning at 600 °C.

The highly organized nature of the prepared silicate-based inverted colloidal crystals is a very attractive feature for fundamental studies of cell interactions. First, one can easily control the porosity of the scaffolds by changing the diameter

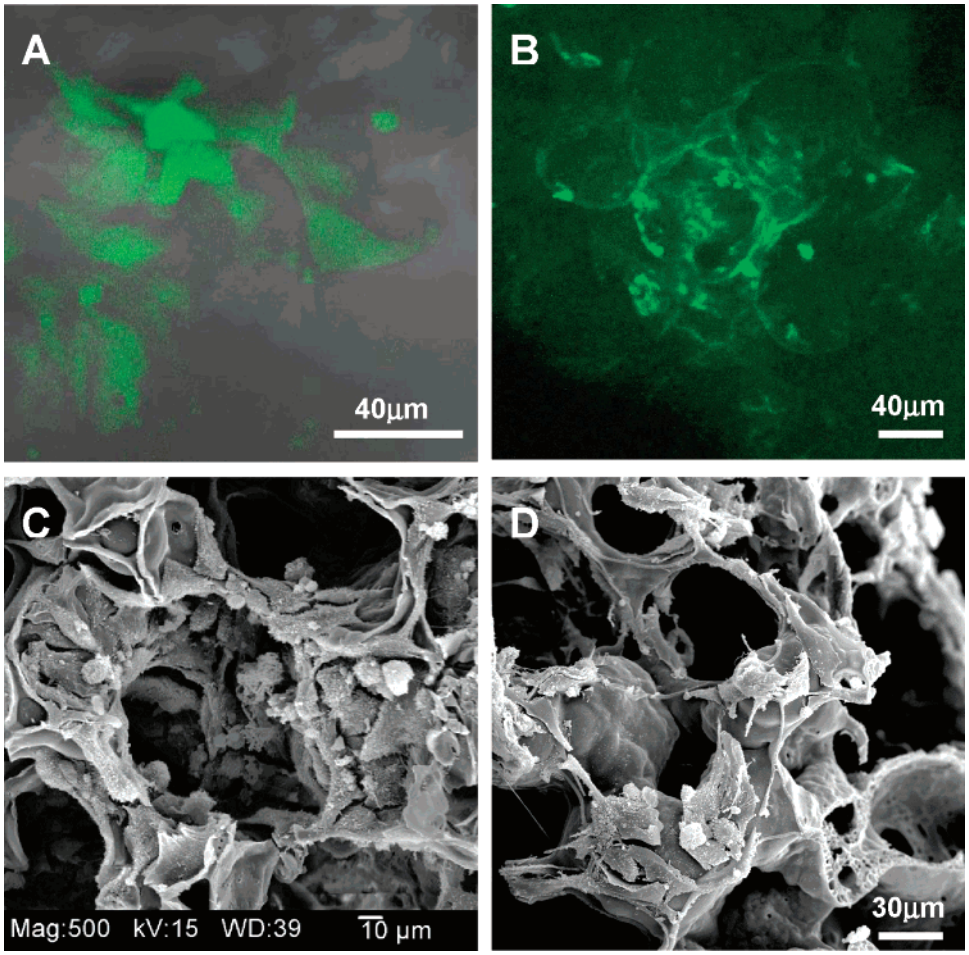

Figure 4. Confocal microscopy and SEM images of 80 μm scaffolds after incubation with a cell culture for 8 days: (A) confocal, HEP G2 cells, (B) confocal HS-5 cells, (C) SEM, HEP G2 cells, (D) SEM, HS-5 cells.

of the starting colloid. Second, the spherical voids left behind by the polymer particles create a highly uniform environment for cell evolution, which simplifies interpretation of the results. Third, the highly ordered structure makes possible computer modeling of the nutrient fluxes, metabolism, cell migration, and other processes on the scaffold, which can hardly be done on chaotic 3D scaffolds.

Regardless of how convenient the structural properties of a scaffold may be, the possible cytotoxicity may render it to be useless. Therefore, one of the most important tasks is the evaluation of the biocompatibility of the scaffolds. As model cell systems, hepatocellular carcinoma HEP G2 and human bone marrow stromal HS-5 cells were selected as in previous studies.[20] Hepatocytes are one of the most sensitive cells to the 3D organization and can be useful for further functional studies.[27] Human bone marrow stromal cells would also be an interesting cell type to test because the morphology of the inverted colloidal crystal scaffolds made here is reminiscent of the internal structure of bone supporting the stromal cells.

Differently sized scaffolds were cultured with HEP G2 cells and HS-5 cells for an identical period of time (8 days). Similar to previous results,[19] HEP G2 cells show high cell density in the scaffolds with pore size equal to or larger than 80 μm, and for the 10 μm pore size scaffold, the cells can only grow on the surface of the scaffold, since the cells cannot fit into the cavities. They are clearly visible in the confocal microscopy image in green in Figure 4A. HS-5 cells also grow well as can be seen in Figure 4B. SEM images (Figure 4C,D) further reveal that the cells grow three-dimensionally along the walls inside the cavities of the scaffolds. These results indicate the inverted colloidal crystal scaffolds can provide a suitable environment for cell growth.

4. Conclusion

We demonstrated a versatile route, the floating self-assembly technique, to prepare differently sized colloidal crystals and the corresponding inverted opals using micro-colloidal particles of sizes 10, 80, 160, and 240 μm. This concise method provides a faster and versatile technique for the preparation of colloidal crystals of micrometer range and can be applied to nanometer and millimeter range. The floating self-assembly may also be expanded to the preparation of many other ordered structures provided that the starting particles have a certain shape and uniform size and that the specific gravity of the solvent is heavier than that of the particles. The prepared inverted colloidal crystals were used as 3D cell scaffolds. Their biocompatibility was confirmed by human hepatocellular carcinoma HEP G2 and human bone marrow HS-5 cell cultures. These scaffolds have

(27) Park, A.; Wu, B.; Griffith, L. *J. Biomater. Sci., Polym. Ed.* **1998**, *9*, 89.

a higher degree of internal order than typical tissue matrixes, making possible the systematic study of the cell interactions and motility.

Acknowledgment. We thank DARPA (DAMD17-02-1-0702 and W81XWH-04-C-0139) and NSF (BES-0119483 for N.A.K.) for support of this research. This research was also supported by an OARS award [AR 03(2)-068] from Oklahoma Center for the Advancement of Science and Technology. S.W. thanks Dr. A. Mamedov for assistance with SEM imaging and Dr. J. Clark, D. Goad, Prof. J. Malayer, and Prof. G. Chen for assistance with the cell cultures. We thank Dr. S. Westcott for proofreading the manuscript and helpful discussions.

CM048050G